Theor Appl Climatol
DOI 10.1007/s00704-016-1905-8

ORIGINAL PAPER

Trends of urban surface temperature and heat island characteristics in the Mediterranean

Nikolaos Benas[1] · **Nektarios Chrysoulakis**[1] · **Constantinos Cartalis**[2]

Received: 22 January 2016 / Accepted: 12 August 2016

Abstract Urban air temperature studies usually focus on the urban canopy heat island phenomenon, whereby the city center experiences higher near surface air temperatures compared to its surrounding non-urban areas. The Land Surface Temperature (LST) is used instead of urban air temperature to identify the Surface Urban Heat Island (SUHI). In this study, the nighttime LST and SUHI characteristics and trends in the seventeen largest Mediterranean cities were investigated, by analyzing satellite observations for the period 2001–2012. SUHI averages and trends were based on an innovative approach of comparing urban pixels to randomly selected non-urban pixels, which carries the potential to better standardize satellite-derived SUHI estimations. A positive trend for both LST and SUHI for the majority of the examined cities was documented. Furthermore, a 0.1 °C decade^{-1} increase in urban LST corresponded to an increase in SUHI by about 0.04 °C decade^{-1}. A longitudinal differentiation was found in the urban LST trends, with higher positive values appearing in the eastern Mediterranean. Examination of urban infrastructure and development factors during the same period revealed correlations with SUHI trends, which can be used to explain differences among cities. However, the majority of the cities examined show considerably increased trends in terms of the enhancement of SUHI. These findings are considered important so as to promote sustainable urbanization, as well as to support the development of heat island adaptation and mitigation plans in the Mediterranean.

✉ Nektarios Chrysoulakis
zedd2@iacm.forth.gr

[1] Foundation for Research and Technology Hellas (FORTH), Institute of Applied and Computational Mathematics, N. Plastira 100, Vassilika Vouton, 70013 Heraklion, Greece

[2] Department of Environmental Physics, National and Kapodistrian University of Athens, Build PHYS-5, 15784 Athens, Greece

1 Introduction

Land Surface Temperature (LST) is a key variable in climatological studies as it has a fundamental role in the exchange of energy between the atmosphere and the Earth's surface in various forms. These forms include long-wave radiation flux, turbulent sensible and latent heat fluxes, and ground heat storage (Chrysoulakis 2003; Weng 2009). LST is used in a variety of scientific fields, from local to global scales, including climate change, energy budget, vegetation monitoring, hydrological cycle and urban climatology (Voogt and Oke 2003; Tomlinson et al. 2011; Sobrino and Julien, 2013; Li et al. 2013). Regarding cities, causes of the Urban Heat Island (UHI) phenomenon are partly natural, because of the differences in land cover and urban form that absorb more solar radiation and trap the long-wave radiation. However, there is also anthropogenic heat release that contributes to increased urban heat, leading to a higher LST equilibrium, and resulting in changes in turbulent sensible and latent heat fluxes, as well as to the long-wave radiation flux. High anthropogenic heat flux values under localized conditions have been reported (Iamarino et al. 2012) and efforts are made to estimate this flux from space (Chrysoulakis et al. 2015). Due to its importance, LST requires continual and intensive spatial and temporal monitoring that can best be achieved consistently for studies of multiple urban areas using satellite observations (Stathopoulou and Cartalis 2007; Li et al. 2013; Yang et al. 2013).

The study of LST in urban environments is highly important also in view of the worldwide urbanization trends and their impacts on climate (Kalnay and Cai 2003). City

Published online: 02 September 2016

population changes are expected to contribute to the urban LST increasing trends, by altering the distribution and intensity of human activities and increasing the anthropogenic heat flux (Stewart and Oke 2012; Clinton and Gong 2013; Georgescu et al. 2014). The main causes of urban warming include the increased impervious surfaces, the large vertical faces of buildings, the reduced sky view factor, the absorption of solar radiation and the emission of thermal radiation by urban materials, as well as the anthropogenic heat flux (Grimmond 2007). Cities have been found not only to exhibit higher nighttime temperatures than nearby rural areas but also, in recent decades, to be warming at a significantly higher rate (Stone 2009; Stone et al. 2012). In fact, elevated urban LST has multiple negative consequences for quality of life, including human health and comfort, air quality and energy consumption. To this end, studying the LST is considered a critical prerequisite for adaptation and mitigation plans (Mackey et al. 2012; Seto and Christensen 2013), as well as for sustainable urban planning (Chrysoulakis et al. 2013, 2014).

In the present study, the nighttime urban LST and corresponding Surface Urban Heat Island (SUHI) were thoroughly analyzed, aiming to quantify their characteristics and trends in the 17 largest Mediterranean cities during the period 2001–2012. For the estimation of SUHI, an innovative approach was developed, whereby LST values from non-urban pixels, required for the computations, are randomly selected from an area surrounding each city. This approach can be used to measure SUHI changes over time, in different geographical regions, thus contributing to standardization of corresponding methodology. Furthermore, several urban development indices were examined in order to gain insight on their possible linkage to SUHI trends. The broader Mediterranean area was selected in this study due to its climatic sensitivity, which has been demonstrated in previous studies; Mediterranean climate change manifestations include decreasing precipitation (Trenberth 2011) and increasing high temperature extremes (Founda and Giannakopoulos 2009), while imminent desertification has also been foreseen by future climatic projections (IPCC 2012). These characteristics, along with high population density, especially in the urban agglomerations of this region, as well as the high importance of the broader study area in terms of human activities and cultural heritage, make monitoring of the urban LST and SUHI in large Mediterranean cities highly significant for studies related to both climatic changes and sustainable urban development.

2 Data and methods

Nighttime LST data, from the Moderate Resolution Imaging Spectroradiometer (MODIS) - Level 3 Version 5 LST 8-day product (MODIS product number: MOD11A2) from NASA's Terra satellite, were used in the present study (Wan 2008). This LST product is made available on a sinusoidal grid at the spatial resolution of about 1 km × 1 km, as the average values of clear sky day and night LSTs, separately, during an 8-day period. This product has been thoroughly validated in the past (Wan 2008; Coll et al. 2009). It should be noted that Terra crosses the equator at around 22:30 local solar time in its nighttime (ascending) mode and MODIS data acquisition at Mediterranean latitudes occurs in a narrow time interval, shortly after the equatorial crossing. Hence, all the nighttime urban LST data and corresponding SUHI estimates (hereinafter LST and SUHI refer always to nighttime) are representative of this time interval, which is however close to the SUHI intensity maxima.

The selection of the 17 Mediterranean cities was based on three criteria: population, city area extent and proximity to the sea. Only cities with population greater than 1,000,000 in 2010 were selected, obtained from the United Nations (UN) World Urbanization Prospects 2014 data (United Nations 2014). For each city, a 30 km × 30 km sampling zone was defined, centered on the corresponding city center. This size was selected to ensure adequate coverage of both urban and rural areas in each city. Geographical coordinates for each city center were retrieved from the UN World Urbanization Prospects data. Urban pixels were discriminated from non-urban ones within the sampling zones, based on land-cover information from the 2009 GlobCOVER V2.3 product (GlobCOVER 2015). This product is available at 0.3 km × 0.3 km spatial resolution from the Medium Resolution Imaging Spectrometer (MERIS) (Bontemps et al. 2011). GlobCOVER comprises 22 land-cover types defined by the United Nations Land Cover Classification System. According to GlobCOVER classification, urban areas are defined as artificial surfaces and associated areas covering more than 50 % of the pixel considered (Bontemps et al. 2011). To upscale the 0.3 km × 0.3 km land-cover data pixels to the 1 km × 1 km LST data, a majority criterion was applied, combined with a nearest neighborhood transformation: the land-cover type assigned to the majority of the land-cover pixels in each LST pixel was used. To estimate representative LST and SUHI characteristics and trends the following criterion was set: at least 100 urban pixels were required to be present in each sampling zone, corresponding to a minimum urban area of 100 km^2. This threshold ensured that cities which met the population criterion, but consisted of relatively few urban pixels (probably due to sparse distribution of buildings, especially in their suburbs), were included in the analysis. A threshold of maximum 150 km Euclidian distance from the sampling zone center to the nearest coast was also applied. This distance was selected in order to include cities near the Mediterranean coast which, although not characterized by a typical Mediterranean climate (Kottek et al. 2006), they are very important in terms of human population and activities (e.g. Cairo). Based on the above criteria of population, urban

pixels in each sampling zone and distance from the coast, the 17 cities that were selected are shown in Fig. 1.

After the acquisition of the LST product time series, covering the period 2001–2012, the 8-day average LSTs were extracted in degrees Celsius as per Wan (2007), for each of the selected Mediterranean cities and for the respective non-urban areas inside the 30 km × 30 km sampling zones. Along with the LST data, the number of nights used for the computation of each 8-day average, available as an 8-bit integer on a pixel basis, was also retrieved and used for the estimation of the annual LST.

The annual means of LST and SUHI would be ideally estimated by averaging the corresponding 8-day products (approximately 46 available in one year). In satellite-derived LST, however, failures in retrieval algorithms are often, caused primarily due to the presence of clouds, which result in gaps in the time series. In order to appropriately take into account these gaps and ensure the representativeness of the calculated annual average, a selection methodology on a pixel basis was developed, which is based on several threshold criteria, and is described in detail in Benas and Chrysoulakis (2015). The criteria applied take into account the number of valid daily LST values in each 8-day product, as mentioned before, and the intra-annual distribution of valid 8-days, to avoid seasonal biases, caused by differences in cloud cover intra-annual distribution. When these criteria were met, the smoothing spline technique (Hutchinson and de Hoog 1985) was applied for the estimation of the annual average. Among several smoothing and gap-filling methods, Musial et al. (2011) showed that this technique is the most appropriate regarding data sets with seasonal patterns and gaps, as in the case of LST.

LST trends (reported in °C decade^{-1}) were assessed on a pixel level, based on the slope of a linear regression analysis, applied to the estimated annual average values during the 12-year period examined. In order to ensure temporal homogeneity in trend values, at least 10 valid annual averages were required, including the first and last years of the time series (2001 and 2012), leading to a maximum of two missing annual averages. Statistical significance of the estimated trends at the 95 % confidence level was also assessed, based on the corresponding confidence intervals of the linear regression slope. Furthermore, the percentage of urban pixels with positive trend was computed in each city to assess the homogeneity and the significance of the city averaged trend.

SUHI is generally defined as the difference of urban LST minus non-urban LST surrounding the city, with urban and non-urban areas covering the same amount of land (e.g. Peng et al. 2012; Zhou et al. 2013). Its definition, however, remains diverse (Schwarz et al. 2011), making comparative assessments across different studies difficult to perform. An innovative approach was developed in the present study, and was used for the estimation of both SUHI time series averages and trends. Based on this approach, the urban LST time series average or trend was estimated as the average of all urban pixels with available corresponding values in the 30 km × 30 km sampling zone. To estimate the corresponding non-urban averaged values, a Monte Carlo approach was employed: a number of non-urban pixels, equal to the number of the urban pixels used before, were randomly selected and

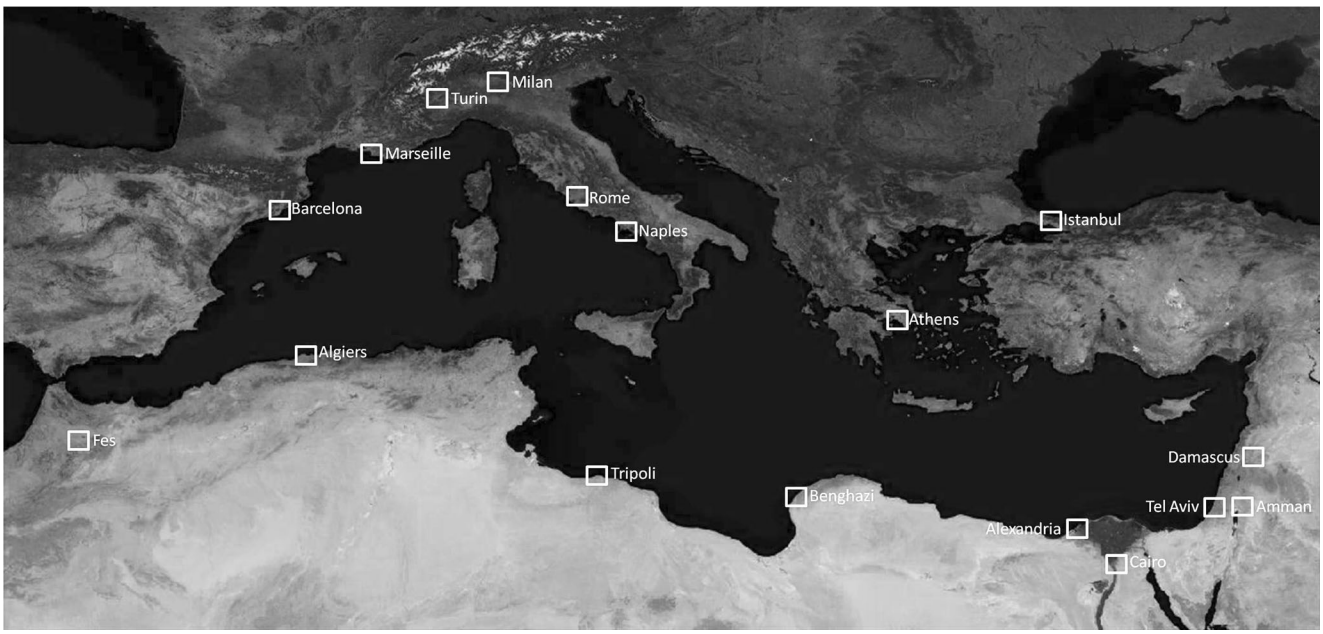

Fig. 1 The broader Mediterranean area and the 17 selected cities. White boxes correspond to 30 km × 30 km sampling zones around each city. (Image credit: NASA)

the average non-urban LST time series average or trend was computed. SUHI time series average or trend was then computed by subtracting the average non-urban value from the average urban value. This methodology requires that the number of non-urban pixels is larger than the number of urban pixels. This was ensured by the selection of the 30 km × 30 km size, whereby urban pixels never exceeded 40 % of the land cover in each sampling zone. This randomization approach overcomes the problems of non-contiguous urban pixels and the resultant requirement of defining clusters of urban pixels and corresponding non-urban buffer zones. In order to account for the different spatial extents of the non-urban land cover types in each sampling zone, which are expected to contribute differently in the overall SUHI, the random non-urban pixels were selected in proportion to the spatial coverage of each land cover type (stratified random selection). The statistical significance of the estimated SUHI average or trend value was assessed based on a permutation test: the urban and the selected non-urban pixels were randomly shuffled into two equal size groups (corresponding to urban and non-urban), and the difference of the average values of these new groups was again estimated. This procedure was repeated 1000 times. The statistical significance of the SUHI average or trend value was then assessed based on the *p*-value, which is computed as the proportion of occurrences of estimated difference values (1000 in total) greater than or equal to the initially estimated value (e.g. Good 2013). The approach developed here carries the potential to better standardize SUHI calculation efforts in different geographic regions and using LST data from different satellite sensors.

For the investigation of the possible effects of human activity changes on SUHI trends, several infrastructure and development indicators, and their changes during the 12-year study period, were examined. These data, including energy consumption and road sector characteristics, are available through the World Bank Development Indicators (World Development Indicators 2014). It should be noted that these data are available on a country level. Hence, examination of their correlation with city-level SUHI trends is based on the assumption that the country-level changes are reflected on the city level. This assumption is expected to hold for major cities in terms of population, since the indicators used are related to human activities. In fact, all cities examined are ranked in the first positions in their countries, in terms of population in 2010. However, the same assumption can also deteriorate correlation results, especially in case of countries with many large cities. For this reason, the effect of population change on SUHI trends was also assessed on a city level, by comparing the population change in each city during the study period, with the respective SUHI trend.

It should also be noted that in coastal cities, sea breeze is among the factors affecting the LST. In fact, it is expected that the sea breeze will influence the observed LST in coastal regions of the sampling zones, while further inland regions will not experience the same effect (e.g. Papanastasiou et al. 2010). Although sea breeze depends on local weather conditions and topography, it shares some common properties around the Mediterranean, including the diurnal and seasonal variations. As mentioned before, the MODIS nighttime data acquisition occurs during a narrow time interval after 22:30 local solar time, which roughly coincides with the sea breeze minimum manifestation (e.g. Cantos and Molina 2004; Papanastasiou et al. 2010). Hence, the corresponding effects are also expected to be minor. In addition, while sea breeze may have significant effects on air temperature, its influence on LST is expected to be less pronounced. The reason is that LST is related to both sensible and latent heat fluxes between the urban surface and the atmosphere, which, as components of the urban energy budget, can be modified by the net advective flux in an urban building–soil–air volume (Roberts et al. 2006). If this net advective flux is caused by sea breeze, then it includes advective fluxes of latent and sensible heat that are of similar size but are opposite in sign, thereby essentially offsetting each other, as indicated by Pigeon et al. (2003). Furthermore, in Mediterranean latitudes sea breeze generally develops during the warm period of the year (e.g. Papanastasiou and Melas 2009). Since the analysis of the present study is based on annual average LST values, this seasonal effect is incorporated in the results. Overall, although sea breeze may be affecting the 8-day average LST values used as input in this study, its influence is not expected to constitute a determinant factor regarding the findings presented here.

3 Results and discussion

3.1 Average LST and SUHI

Figure 2 shows an example of the land cover type map in the wider area of Barcelona, along with the 2001–2012 averaged LST and LST trends for the same period. The city area extent and the surrounding urban agglomerations are clearly shown (red pixels in the left map of Fig. 2). It is also apparent from the average LST map, that urban areas generally exhibit higher LST compared to non-urban, leading to a SUHI of ~1 °C (also shown in Table 1). A positive LST trend (right map of Fig. 2) was found for 82 % of the urban pixels (Table 2), while mixed signs were found in non-urban areas, leading to an overall increase of ~0.1 °C per decade for urban LST and SUHI.

Table 1 shows the temporally and spatially averaged urban LST and SUHI for the selected Mediterranean cities, presented from west to east. The latitudinal effect on the average LST is apparent, with the highest values appearing in cities of Northern Africa (Cairo and Alexandria) and the lowest in cities of Southern Europe, located in higher latitudes (Turin

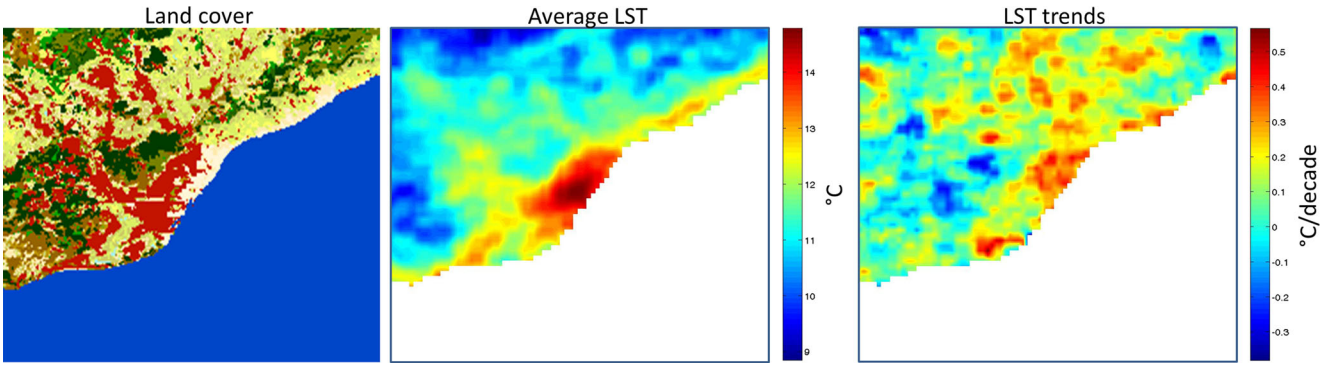

Fig. 2 Land cover type map of the Barcelona wider area (left), with urban pixels shown in red; the 2001–2012 average nighttime LST (middle) and the nighttime LST trends (right) are also shown. The middle and left images were smoothed using a 3 × 3 pixel averaging filter

and Milan). Apart from the latitudinal effect, LST in these two Italian cities may also be affected by the proximity to the Alps. However, although the latitudinal effect is verified by the high correlation ($R^2 = 0.86$) found between latitude and averaged urban LST data, no correlation was found when the latter were compared against altitude and distance to the sea. The LST standard deviations reflect the spatial variability of the LST distribution in each city. In all cases, the LST variation among urban pixels lies around ±1 °C and should probably be attributed to locations within the city with significantly different land cover. SUHI also varies significantly among the 17 cities studied, however its values are relatively small, as they represent average annual values, thus they encompass all seasons and not only summer, when SUHI obtains its highest values.

Table 1 Spatially and temporally averaged urban LST and SUHI in the 17 cities. LST standard deviations correspond to the spatial average, while SUHI *p*-values show the proportion of occurrences, in the permutation tests, of SUHI values greater than or equal to the estimated SUHI

City	LST (°C)	SUHI (°C) (p-value)
Fes	13.89 ± 1.06	0.78 (0.00)
Algiers	14.02 ± 0.73	1.43 (0.00)
Barcelona	12.13 ± 1.04	1.04 (0.00)
Marseille	11.23 ± 0.85	1.31 (0.00)
Turin	9.00 ± 1.37	1.83 (0.00)
Milan	9.39 ± 0.97	1.08 (0.00)
Rome	11.48 ± 1.13	1.54 (0.00)
Naples	12.01 ± 0.70	0.90 (0.00)
Tripoli	15.85 ± 1.02	1.44 (0.00)
Benghazi	16.48 ± 0.63	1.27 (0.00)
Athens	14.02 ± 1.32	1.78 (0.00)
Istanbul	11.68 ± 0.41	0.74 (0.00)
Alexandria	18.51 ± 0.94	3.47 (0.00)
Cairo	19.62 ± 1.09	2.83 (0.00)
Tel Aviv	16.16 ± 1.10	0.83 (0.00)
Amman	13.74 ± 0.72	0.02 (0.94)
Damascus	15.28 ± 0.85	3.94 (0.00)

For southern European cities SUHI ranges between 0.74 °C (Istanbul) and 1.83 °C (Turin), while values in the range 1.2–1.5 °C are found in three northern African cities (Algiers, Tripoli and Benghazi), which are surrounded by a mosaic of croplands and vegetation combined with desert patches. The highest SUHI values appear in Damascus, Alexandria and Cairo, and should probably be attributed to desert areas surrounding the cities, with low nighttime LST which increases the SUHI intensity. The SUHI *p*-values in Table 1 show that, with the exception of Amman, all the estimated SUHIs are

Table 2 Indicators of representativeness of the averaged LST trends, and p-values computed from the permutation tests on SUHI trends. Indicators include percentage of total urban pixels used in the computations, percentage of used pixels with statistically significant trends and percentage of used pixels with positive trends

City	Urban pixels used in LST trends computation (%)	Urban pixels with statistically significant LST trend (%)	Urban pixels with positive LST trend (%)	P-values of SUHI trends
Fes	100	21.0	94.7	0
Algiers	100	33.0	100	0
Barcelona	100	0.0	82.0	0
Marseille	96.2	0.0	38.5	0.58
Turin	56.5	2.2	74.8	0.83
Milan	100	0.3	84.5	0.02
Rome	99.3	0.1	92.3	0
Naples	98.0	7.4	94.3	0.01
Tripoli	99.9	93.9	100	0
Benghazi	99.6	15.9	99.8	0
Athens	93.6	0.8	100	0.07
Istanbul	48.1	1.4	72.7	0
Alexandria	92.5	38.1	99.5	0.10
Cairo	96.5	93.9	100	0.01
Tel Aviv	100	19.5	100	0
Amman	100	19.4	100	0
Damascus	100	2.1	100	0

statistically significant at the 99 % confidence interval. In the case of Amman, the practically absent SUHI effect should be attributed to the high LST variability caused by the variation in land-cover types and surface morphology in the sampling zone: while the city is warmer than its immediate surroundings, which are characterized mainly by sparse vegetation, the sampling zone includes desert areas (low nighttime LST) and mountainous areas facing west (high LST values in the afternoon and therefore during the satellite acquisition time).

3.2 LST and SUHI trends

The urban LST trends were first computed on a pixel basis and then averaged. Hence, as in the average LST case, standard deviations reflect the spatial variability of the LST trends in each city. This approach was selected in order to allow a more in-depth investigation of the homogeneity and severity of the trend results inside each city, which were assessed based on the percentages of urban pixels used within the total urban area, those with positive LST trends and those with statistically significant LST trends (Table 2). The averaged LST trends in each city, with their corresponding standard deviations, are shown in Fig. 3. With the exception of Marseille, averaged LST trends in most cities are positive. It is also apparent that moving eastwards, trends tend to increase. Although synoptic scale effects may be among the reasons causing this tendency, as also suggested by the correlation between latitude and LST trends ($R^2 = 0.64$), differences among countries on development indicators, presented below, also appear explanatory of this increase. As shown in Table 2, the urban pixels used in the trends calculations, after applying the thresholds described in Section 2, exceed 90 % of the total urban area (total number of urban pixels according to GlobCOVER data) in 15 of the 17 cities, reaching full and almost full coverage (over 99 %) in 10 of them. The lowest coverage (about 50 %) appears in Turin and Istanbul. This sparse coverage presumably causes the large LST standard deviations in these two cities (Fig. 3). Another interesting finding is the high percentage of urban pixels with positive LST trend, which exceeds 80 % in 14 of the 17 cities. Although in most cities statistically significant increasing trends on a pixel basis cover relatively small areas (see Table 2), the previous finding suggests a spatially homogeneous tendency of increasing LSTs in 16 of the 17 cases. In fact, the urban LST trends found in some of the examined cities appear considerably increased in terms of the state of their thermal environment, highlighting the need of increased awareness regarding climate adaptation and mitigation plans.

The results of the SUHI trends analysis are shown in Fig. 4. With the exception of four cities (Marseille, Turin, Athens and Alexandria), SUHI trends were found statistically significant at the 95 % confidence interval. Statistically significant SUHI trends with low values (e.g. in Milan and Naples) should probably be attributed to spatial homogeneity in LST trends of both urban and non-urban pixels. It is highly improbable that randomly reshuffled pixels in the two new groups during the permutation tests will exhibit the same homogeneity; this will lead to low *p*-values and hence statistically significant SUHI trends. The highest values of SUHI trends, in the range 0.14–0.39 °C decade^{-1}, appear in cities of Northern Africa and the Middle East. Low absolute SUHI trend values, on the other hand, are found in cities of both Northern Africa and Europe. In the case of European cities, low SUHI values combined with the low LST trend values, show that there are relatively stable LST conditions in these areas, during the

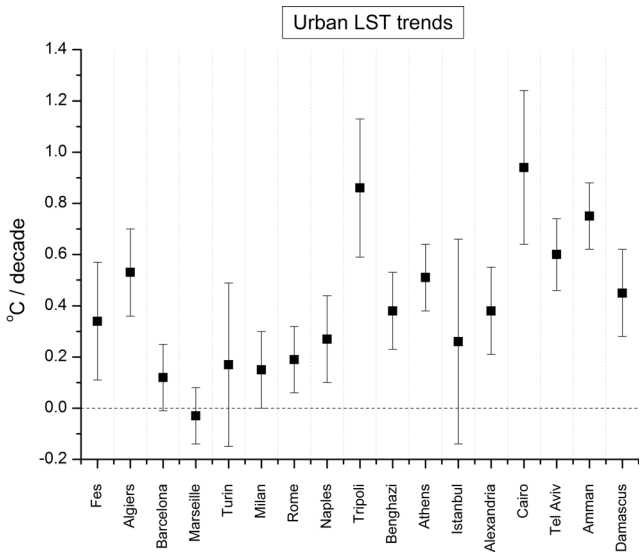

Fig. 3 Averaged urban LST trends in the selected Mediterranean cities, in °C decade^{-1}, computed from the 12-year time series. Error bars represent the corresponding standard deviations. Cities are arranged in the X-axis from west to east

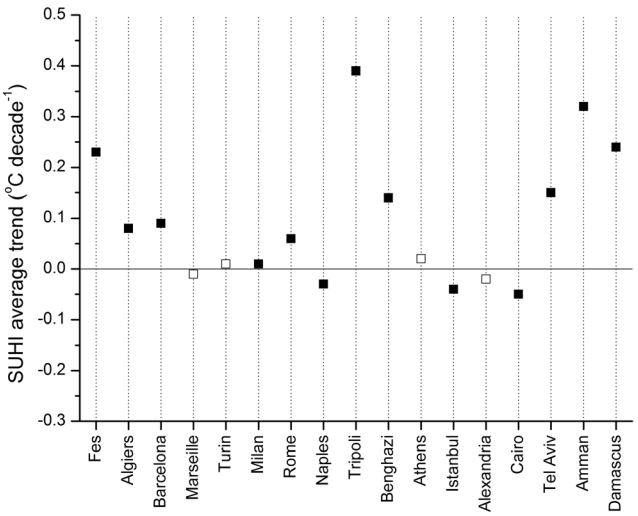

Fig. 4 SUHI average trends (in °C decade^{-1}) in the selected Mediterranean cities. Statistically significant trends are shown in black squares. Vertical dotted lines are included for clarity purposes. Cities are arranged from west to east

period examined. As noted before, with the exception of Marseille, urban LST trends are positive. Hence, the statistically significant negative SUHI trends found in Naples, Istanbul and Cairo should not be attributed to cooling trends inside the urban areas. They were instead caused by more rapidly increasing LSTs in non-urban pixels surrounding these cities, compared to the corresponding urban LST trends.

It is also worth noting that SUHI trends are well correlated with urban LST trends, with the exception of Cairo. While Cairo exhibits the highest LST trend, a negative SUHI trend is found, due to a faster warming of the non-urban areas, as mentioned before. Figure 5 shows a scatter-plot of the LST trend vs. the SUHI trend in the 17 Mediterranean cities and the corresponding linear regression fit. If Cairo, which acts as an outlier in the plot, is excluded from the regression, the correlation coefficient substantially increases and also becomes statistically significant at the 95 % confidence interval. This correlation implies that in most cases, when the urban LST increases, the SUHI also increases. As a general rule, based on the linear regression equation, a 0.1 °C decade^{-1} increase in urban LST is correlated with an increase in SUHI by about 0.04 °C decade^{-1}.

The correlation between urban LST and SUHI trends, combined with the above mentioned differences between European cities and cities in northern Africa and the Middle East, suggest that differences and changes in urban structures and human activities constitute important driving factors of the trends presented here. While urban sprawl can be among these factors, precise land cover change detection requires higher spatial resolution (30 m or better) compared to the 1 km used here (Bontemps et al. 2012b). In the framework of the present study, different land cover products at 1 km × 1 km resolution, which span the 2001–2012 study period, were examined, including the MODIS Land Cover (Friedl et al. 2010) and the European Space Agency Climate Change Initiative (ESA CCI) Land Cover products (Bontemps et al. 2012a, b); no changes in urban extents were detected in either product. For similar reasons, the effect of intra-urban land cover variation cannot be analyzed at this spatial resolution, although it is expected to contribute in corresponding variations of both LST and SUHI characteristics and trends.

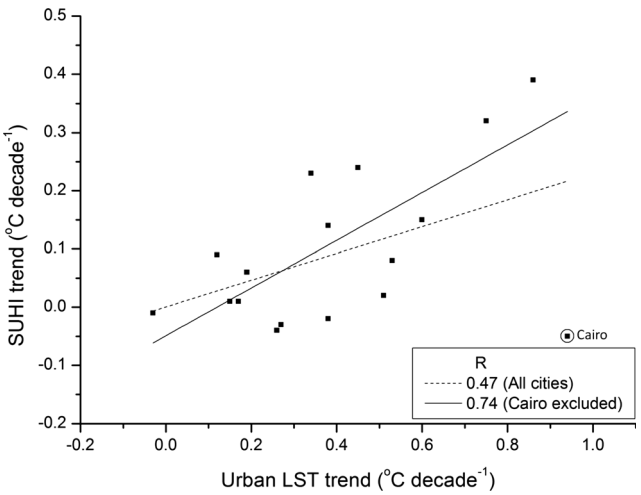

Fig. 5 The scatter-plot shows the LST trends vs. the SUHI trends for the 17 Mediterranean cities examined. The linear regression fits and the correlation coefficients, applied to all cities (dashed line) and to all cities excluding Cairo (solid line) are also shown. In most cases an increase in urban LST is correlated with an increase in the respective SUHI

A multiple regression approach was used for the examination of the effects of urban development (as described by the indicators in Table 3) on SUHI trends, whereby the percent changes of these indicators during the study period were used as the predictor variables and SUHI trends (for all cities under study) as the response variable. Results show good correlation, with an adjusted R^2 equal to 0.76 and most of the *p*-values, for each of the above indicators, revealing statistical significance at the 95 % confidence interval, as shown in Table 3. The poor performance of electric power consumption could be attributed to the complexity of power grids, with exchanges of power across cities and countries that may be reducing the predictive efficiency of this indicator. Indices related to the road sector energy consumption and traffic density, which include motor vehicles and passenger cars, on the other hand, appear to contribute to the SUHI trends, presumably by increasing the urban LST. Major increases of these indices during the period examined were found in northern Africa and Middle East countries, which should probably be attributed to their higher development rates, compared to SW European countries. These geographic variations are also reflected in SUHI trends, as shown in Fig. 4. These findings imply that these or similar indicators, referring primarily to road sector changes, could contribute to long-term SUHI changes. A relatively poor performance appears in the case of the percentage of urban population (Table 3). Further investigation revealed discrepancies between this indicator and SUHI trends, which can explain this performance; these include cases of increase in urban population that was not accompanied by similar increase in SUHI and vice versa. The comparison of SUHI trends with city-level urban population changes (Table 4) also resulted in poor overall correlation (R = 0.28), as expected due to differences in regional climatic conditions, city structures and human activities. It was found, however, that some neighboring cities can be grouped. The four Italian cities, along with Marseille, exhibit similar behavior: the city population changes were small (and negative in three cases), and the corresponding SUHI changes were insignificant. Alexandria and Cairo can also be grouped in terms of SUHI trends and population changes. Although the results for these two cities appear counter-intuitive, with increasing populations and

Table 3 Development indices examined as drivers of SUHI changes. Descriptions of each index, along with the source of corresponding data are provided. The p-values computed using the multiple regression approach are also shown

Indicator	Description	Data Source	P-value
Electric power consumption (kWh per capita)	Production of power plants and combined heat and power plants less transmission, distribution, and transformation losses and own use by heat and power plants.	International Energy Agency[a]	0.241
Motor vehicles (per 1000 people)	Include cars, busses, and freight vehicles.	International Road Federation, World Road Statistics and data files[b]	0.008
Passenger cars (per 1000 people)	Road motor vehicles, other than two-wheelers, intended for the carriage of passengers.	International Road Federation, World Road Statistics and data files[c]	0.031
Road sector energy consumption (% of total energy consumption)	Total energy used in the road sector including petroleum products, natural gas, electricity, and combustible renewable and waste. Total energy consumption is the total country energy consumption.	International Road Federation and International Energy Agency[d]	0.009
Urban population (% of total)	People living in urban areas as defined by national statistical offices. It is calculated using World Bank population estimates and urban ratios from the United Nations World Urbanization Prospects.	United Nations, World Urbanization Prospects[e]	0.162

[a] Available online at http://data.worldbank.org/indicator/EG.USE.ELEC.KH.PC/countries. Accessed 11 December 2015

[b] Available online at http://data.worldbank.org/indicator/IS.VEH.NVEH. P3/countries. Accessed 11 December 2015

[c] Available online at http://data.worldbank.org/indicator/IS.VEH.PCAR. P3/countries. Accessed 11 December 2015

[d] Available online at http://data.worldbank.org/indicator/IS.ROD.ENGY.ZS/countries. Accessed 11 December 2015

[e] Available online at http://data.worldbank.org/indicator/SP.URB.TOTL.IN.ZS/countries. Accessed 11 December 2015

decreasing SUHIs, further investigation showed that the negative trends in SUHI should be attributed to desert areas surrounding these cities, where LST increased more rapidly compared to the urban areas.

Table 4 SUHI trends (in °C decade^{-1}) and population changes (in percent) in the 17 Mediterranean cities. Two distinct groups of cities (the four cities of Italy and Marseille, and the two cities of Egypt) are shown in Italic

City	SUHI trend (°C decade^{-1})	Population change (%)
Fes	0.23	14.9
Algiers	0.08	21.8
Barcelona	0.09	7.9
Marseille	*-0.01*	*2.9*
Turin	*0.01*	*-2.4*
Milan	*0.01*	*-1.3*
Rome	*0.06*	*-1.2*
Naples	*-0.03*	*0.9*
Tripoli	0.39	16.5
Benghazi	0.14	25.5
Athens	0.02	1.9
Istanbul	-0.04	15.1
Alexandria	*-0.02*	*15.6*
Cairo	*-0.05*	*12.9*
Tel Aviv	0.15	13.1
Amman	0.32	5.0
Damascus	0.24	21.1

The latter finding highlights the importance of natural factors acting as drivers of LST and SUHI changes. In fact, although the role of anthropogenic heat on SUHI was examined here separately, its importance should also be viewed relative to its corresponding role in LST; the anthropogenic heat is mainly released as sensible heat, thus contributing to the increase of air temperature, and therefore to smoothing of the temperature gradient between the urban surface and the canopy layer. For this reason, the anthropogenic heat has a positive feedback on LST. Although the LST is mainly defined by the urban surface morphology and cover, the role of the anthropogenic heat release is significant for the LST regime in cases of relatively high anthropogenic heat flux compared to the net all-wave radiation, since both are inputs in the urban energy budget. Such cases include, among others, peak hours and industrial areas (e.g. Chrysoulakis et al. 2015, Chrysoulakis and Grimmond 2016).

4 Conclusions

The urban LST and SUHI characteristics and trends were estimated at 17 large Mediterranean cities during the period 2001–2012, using MODIS 1 km × 1 km data. An innovative randomization method was developed for the estimation of SUHI time series and trends. The method combines LST and land cover data, and contributes to a better standardization of satellite-derived SUHI estimations. The analysis showed generally increasing LST trends in the majority of

cities and large variations in SUHI trends, which appear to correlate with urban development indicators, especially changes related to road sector activities.

While LST changes mainly depend on natural factors, these results highlight the importance of detailed examination of the characteristics of the urban stock, of the variation of the anthropogenic heat flux inside the cities, as well as of the prevailing mechanisms related to microclimate and heat transfer. Findings also demonstrate the need for heat island adaptation and mitigation plans and for detailed microclimatic and energy budget studies prior to any major urban intervention. In the case of Mediterranean cities, this need is further enhanced due to the climatic sensitivity of the area as linked to the high population density and the urbanization trends. Fine spatial resolution satellite observations have the potential to support adaptation and mitigation plans at local scale. Such observations can be combined with urban climate models so as to simulate the impact of the heat island mitigation strategies on urban thermal status in a city as a whole, as well as in neighborhood level. To this end, future operational satellite missions, such as the Copernicus Sentinels series, are expected to further enhance the potential of Earth Observation to analyze the urban LST and SUHI trends. In particular, exploitation of information on high resolution surface cover data from MSI (Multispectral Instrument) on board Sentinel 2 satellite, is expected to provide frequent (daily) LST estimates at local scale, by downscaling SLSTR (Sea and Land Surface Temperature Radiometer, on board Sentinel 3) thermal infrared observations, as in Mitraka et al. (2015). In this way, the intra-urban LST variability can be assessed, enabling the identification of urban heat island and SUHI based on Local Climate Zones, as recently suggested by Stewart and Oke (2012).

Acknowledgments This work was performed in the framework of the PEFYKA project within the KRIPIS Action of the GSRT. The project is funded by Greece and the European Regional Development Fund of the European Union under the NSRF and the O.P. Competitiveness and Entrepreneurship. The MODIS MOD11A2 product files were obtained from the NASA Land Processes Distributed Active Archive Center (https://lpdaac.usgs.gov/dataset_discovery/modis/modis_products_table/mod11a2). The GlobCOVER V2.3 product files were obtained from the ESA Data User Element web page (http://due.esrin.esa.int/page_globcover.php).

References

Benas N, Chrysoulakis N (2015) Estimation of the land surface albedo changes in the broader Mediterranean area, based on 12 years of satellite observations. Remote Sens 7(12):16150–16163. doi:10.3390/rs71215816

Bontemps S, Defourny P, Brockmann C, Herold M, Kalogirou V, Arino O (2012a) New global land cover mapping exercise in the framework of the ESA climate change initiative. Geoscience and remote sensing symposium (IGARSS), 2012. IEEE Int:44–47. doi:10.1109/IGARSS.2012.6351640

Bontemps S, Defourny P, Van Bogaert E, Arino O, Kalogirou V, Perez JR (2011) GLOBCOVER 2009: Products description and validation report. European Space Agency and Université catholique de Louvain

Bontemps S, Herold M, Kooistra L, Van Groenestijn A, Hartley A, Arino O, Moreau I, Defourny P (2012b) Revisiting land cover observation to address the needs of the climate modeling community. Biogeosciences 9:2145–2157. doi:10.5194/bg-9-2145-2012

Cantos JO, Molina CA (2004) The meteorological importance of sea-breezes in the Levant region of Spain. Weather 59:282–286. doi:10.1256/wea.176.03

Chrysoulakis N (2003) Estimation of the all-wave urban surface radiation balance by use of ASTER multispectral imagery and in situ spatial data. J Geophys Res 108:4582. doi:10.1029/2003JD003396

Chrysoulakis N et al. (2013) Sustainable urban metabolism as a link between bio-physical sciences and urban planning: the BRIDGE project. Landsc Urban Plan 112:100–117. doi:10.1016/j.landurbplan.2012.12.005

Chrysoulakis N et al. (2014) A conceptual list of indicators for urban planning and management based on earth observation. ISPRS Int J Geo-Inf 3:980–1002

Chrysoulakis N et al (2015) A novel approach for anthropogenic heat flux estimation from space. Proceedings of the 9th International Conference on Urban Climate jointly with 12th Symposium on the Urban Environment, Toulouse, France

Chrysoulakis N, Grimmond CSB (2016) Understanding and reducing the anthropogenic heat emission. In: Santamouris M, Kolokotsa D (eds) Urban Climate Mitigation Techniques. Routledge, Taylor & Francis, London ISBN 978–0-415–71213–2, pp. 27–39

Clinton N, Gong P (2013) MODIS detected surface urban heat islands and sinks: global locations and controls. Remote Sens Environ 134:294–304. doi:10.1016/j.rse.2013.03.008

Coll C, Wan Z, Galve JM (2009) Temperature-based and radiance-based validations of the V5 MODIS land surface temperature product. J Geophys Res 114:D20102. doi:10.1029/2009JD012038

Founda D, Giannakopoulos C (2009) The exceptionally hot summer of 2007 in Athens, Greece – atypical summer in the future climate? Glob Planet Change 67:227–236

Friedl MA, Sulla-Menashe D, Tan B, Schneider A, Ramankutty N, Sibley A, Huang X (2010) MODIS collection 5 global land cover: algorithm refinements and characterization of new datasets. Remote Sens Environ 114:168–182. doi:10.1016/j.rse.2009.08.016

Georgescu M, Morefield PE, Bierwagen BG, Weaver CP (2014) Urban adaptation can roll back warming of emerging megapolitan regions. Proc Natl Acad Sci U S A 111:2909–2914. doi:10.1073/pnas.1322280111

GlobCOVER ESA Data User Element. http://due.esrin.esa.int/page_globcover.php. Accessed 10 November 2015

Good P (2013) Permutation tests: a practical guide to Resampling methods for testing hypotheses. Springer Series in Statistics, Springer New York

Grimmond CSB (2007) Urbanization and global environmental change: local effects of urban warming. Geogr J 173:83–88. doi:10.1111/j.1475-4959.2007.232_3.x

Hutchinson MF, de Hoog FR (1985) Smoothing noisy data with Spline functions. Numer Math 47:99–106

Iamarino M, Beevers S, Grimmond CSB (2012) High-resolution (space, time) anthropogenic heat emissions: London 1970 - 2025. Int J Climatol 32(11):1754–1767. doi:10.1002/joc.2390

IPCC (2012) Managing the risks of extreme events and disasters to advance climate change adaptation. A special report of working groups I and II of the intergovernmental panel on climate change. Cambridge University Press, Cambridge, UK, and New York, NY, USA

Kalnay E, Cai M (2003) Impact of urbanization and land-use change on climate. Nature 423:528–531

Kottek M, Grieser J, Beck C, Rudolf B, Rubel F (2006) World map of the Köppen-Geiger climate classification updated. Meteorol Z 15:259–263. doi:10.1127/0941-2948/2006/0130

Li ZL, Tang BH, Wu H, Ren H, Yan G, Wan Z, Trigo IF, Sobrino JA (2013) Satellite-derived land surface temperature: current status and perspectives. Remote Sens Environ 131:14–37. doi:10.1016/j.rse.2012.12.008

Mackey CW, Lee X, Smith RB (2012) Remotely sensing the cooling effects of city scale efforts to reduce urban heat island. Build Environ 49:348–358. doi:10.1016/j.buildenv.2011.08.004

Mitraka Z, Chrysoulakis N, Doxani G, Del Frate F, Berger M (2015) Urban surface temperature time series estimation at the local scale by spatial-spectral unmixing of satellite observations. Remote Sens 7(4):4139–4156. doi:10.3390/rs70404139

Musial JP, Verstraete MM, Gobron N (2011) Technical note: comparing the effectiveness of recent algorithms to fill and smooth incomplete and noisy time series. Atmos Chem Phys 11:7905–7923. doi:10.5194/acp-11-7905-2011

Papanastasiou DK, Melas D (2009) Climatology and impact on air quality of sea breeze in an urban coastal environment. Int J Climatol 29:305–315. doi:10.1002/joc.1707

Papanastasiou DK, Melas D, Bartzanas T, Kittas C (2010) Temperature, comfort and pollution levels during heat waves and the role of sea breeze. Int J Biometeorol 54:307–317. doi:10.1007/s00484-009-0281-9

Peng S, Piao S, Ciais P, Friedlingstein P, Ottle C, Breon FM, Nan H, Zhou L, Myneni RB (2012) Surface urban heat island across 419 global big cities. Environ Sci Technol 46:696–703. doi:10.1021/es2030438

Pigeon G, Lemonsu A, Masson V, Durand P (2003) Sea–town interactions over Marseille-Part II: Consequences on atmospheric structure near the surface. Proc of the 5th Int Conf on Urban Climate, Lodz, Poland

Roberts SM, Oke TR, Grimmond CSB, Voogt JA (2006) Comparison of four methods to estimate urban heat storage. J Appl Meteorol Climatol 45:1766–1781. doi:10.1175/JAM2432.1

Schwarz N, Lautenbach S, Seppelt R (2011) Exploring indicators for quantifying surface urban heat islands of European cities with MODIS land surface temperatures. Remote Sens Environ 115(12):3175–3186

Seto KC, Christensen P (2013) Remote sensing science to inform urban climate change mitigation strategies. Urban Climate 3:1–6. doi:10.1016/j.uclim.2013.03.001

Sobrino JA, Julien Y (2013) Time series corrections and analyses in thermal remote sensing. In: Kuenzer C, Dech S (eds) Thermal infrared remote sensing: sensors. Methods, Applications. Springer, pp. 267–285

Stathopoulou M, Cartalis C (2007) Use of satellite remote sensing in support of urban heat island studies. Adv Build Energy Res 1:203–212. doi:10.1080/17512549.2007.9687275

Stewart ID, Oke TR (2012) Local climate zones for urban temperature studies. Bull Am Meteor Soc 93:1879–1900. doi:10.1175/BAMS-D-11-00019.1

Stone B (2009) Land use as climate change mitigation. Environ Sci Technol 43:9052–9056. doi:10.1021/es902150g

Stone B, Vargo J, Habeeb D (2012) Managing climate change in cities: will climate action plans work? Landsc Urban Plan 107:263–271. doi:10.1016/j.landurbplan.2012.05.014

Tomlinson CJ, Chapman L, Thornes JE, Bakera C (2011) Remote sensing land surface temperature for meteorology and climatology: a review. Meteor Appl 18:296–306. doi:10.1002/met.287

Trenberth KE (2011) Changes in precipitation with climate change. Clim Res 47:123–138. doi:10.3354/cr00953

United Nations, Department of Economic and Social Affairs, Population Division (2014) World Urbanization Prospects: The 2014 Revision, Highlights (ST/ESA/SER.A/352)

Voogt JA, Oke TR (2003) Thermal remote sensing of urban climates. Remote Sens Environ 86:370–384. doi:10.1016/S0034-4257(03)00079-8

Wan Z (2007) Collection-5 MODIS Land Surface Temperature Products Users' Guide. Institute for Computational Earth System Science, University of California, Santa Barbara, CA, USA

Wan Z (2008) New refinements and validation of the collection-6 MODIS land-surface temperature/emissivity product. Remote Sens Environ 112:59–74. doi:10.1016/j.rse.2013.08.027

Weng Q (2009) Thermal infrared remote sensing for urban climate and environmental studies: methods, applications, and trends. ISPRS J Photogramm 64:335–344. doi:10.1016/j.isprsjprs.2009.03.007

World Development Indicators (2014) http://data.worldbank.org/data-catalog/world-development-indicators. Accessed 11 December 2015

Yang J, Gong P, Fu R, Zhang M, Chen J, Liang S, Xu B, Shi J, Dickinson R (2013) The role of satellite remote sensing in climate change studies. Nat Clim Chang 3:875–883. doi:10.1038/nclimate1908

Zhou B, Rybski D, Kropp JP (2013) On the statistics of urban heat island intensity. Geophys Res Lett 40:5486–5491. doi:10.1002/2013GL057320